

Influence of Process Parameters on the Electrochemical Properties of Hierarchically Structured $\text{Na}_3\text{V}_2(\text{PO}_4)_3/\text{C}$ Composites

Marcel Häring,^[a] Holger Geßwein,^[a] Nicole Bohn,^[a] Helmut Ehrenberg,^[a] and Joachim R. Binder^{*[a]}

Sodium vanadium phosphate $\text{Na}_3\text{V}_2(\text{PO}_4)_3$ (NVP) is a promising next-generation cathode material for sodium-ion batteries (SIB) but the practical application as a cathode active material for SIBs is hindered by its poor electronic conductivity. To overcome this limitation and to improve the electrochemical performance in terms of rate capability and cycling stability, carbon coatings are a viable approach. In this work, we utilized

a spray-drying synthesis process and systematically varied the processing parameters to optimize the electrochemical performance of NVP/carbon composite materials. The spray-drying process yields spherical, porous granules of NVP particles embedded in a carbon matrix, which is formed by the thermal decomposition of polyacrylic acid or β -lactose.

Introduction

Sustainability is an essential criterion for the evaluation of energy storage concepts due to the constantly increasing environmental pollution. In this context electrochemical energy storage gained in importance during the last decade.^[1] The most used system in such applications is the lithium ion battery (LIB) technology. Due to the uprising exploitation of electrochemical energy storage systems and the increasing cost of lithium, it is important to consider alternatives.^[2] Reasons for the high cost of lithium are the special distribution location of lithium resources and the limited reserves.^[3–5] One alternative is the sodium-ion battery (SIB), which has a similar electrochemical storage mechanism to the LIB.^[1,6] An advantage of this system is the high abundance of sodium-salts in the earth crust and in the oceans. For a technology change, it is essential to develop well-suited materials for all battery components. A promising candidate for the application as cathode material is $\text{Na}_3\text{V}_2(\text{PO}_4)_3$ (NVP) which exhibits high energy and power density as well as an excellent rate performance.^[7,8] Nevertheless, NVP suffers from low electronic conductivity. There exist several approaches to enhance the electrochemical properties of NVP materials. One promising strategy is the incorporation of dopants into the NASICON crystal structure. Xu et al. demonstrated, that doping low amounts of cost-efficient

Fe^{2+} ions activates the $\text{V}^{4+}/\text{V}^{5+}$ redox, which leads to a large reversible capacity of 133 mAh g^{-1} .^[9] Multicomponent doping of Cr and Si^{10} or the combined approach of carbon coating together with Nb^{5+} substitution into the crystal structure^[11] recently proved the enhancement of the electronic conductivity of NVP composites. Beside this crystal-chemical modification of the NASICON structures, a different viable approach is microstructure engineering. Embedding the cathode-active NVP material into a carbon matrix^[12,13] or shortening the diffusion paths lengths by the synthesis of smaller particles,^[14,15] both improve the electronic conductivity. Improvements of the electrochemical cycling stability can be achieved by the generation of porous structures to buffer the volume expansion during sodium-ion insertion.^[16,17] The best way to handle the combination of all mentioned approaches is the synthesis of hierarchically structured materials.^[18–20] In accordance, hierarchically porous $\text{Na}_3\text{V}_2(\text{PO}_4)_3/\text{C}$ composites with capacities up to 113 mAh/g capacity retentions up to 88% were synthesized previously.^[21,22] Spray-drying is an established method to synthesize hierarchically structured porous materials.^[23,24] In this work, we synthesized hierarchically structured $\text{Na}_3\text{V}_2(\text{PO}_4)_3/\text{C}$ composites with defined microstructures via a spray-drying process. We show how the variation of different synthesis parameters, such as carbon content, calcination temperature and atmosphere or degree of milling influence the electrochemical performance. After the optimization by the variation of the parameters, we reached capacities up to 109 mAh/g with a capacity retention of 98.4% after 275 cycles.

Results and Discussion

Variation of the synthesis and processing parameters

Most Na^+ superionic conductor (NASICON) materials, including the vanadium based NVP, exhibit poor electronic conductivity

[a] M. Häring, Dr. H. Geßwein, N. Bohn, Prof. H. Ehrenberg, Dr. J. R. Binder
Institute for Applied Materials, Karlsruhe Institute of Technology
Hermann-von-Helmholtz-Platz 1, 76344 Eggenstein-Leopoldshafen (Germany)
E-mail: joachim.binder@kit.edu

Supporting information for this article is available on the WWW under
<https://doi.org/10.1002/celec.202300401>

© 2023 The Authors. ChemElectroChem published by Wiley-VCH GmbH. This is an open access article under the terms of the Creative Commons Attribution License, which permits use, distribution and reproduction in any medium, provided the original work is properly cited.

and therefore some kind of electronic conducting material such as carbon has to be added for the use as a cathode active material for SIBs.^[25] To investigate the influence of different carbon contents on the electrochemical performance we synthesized two NVP/carbon precursors with varying carbon contents (NVP-lowC-Pre and NVP-C-Pre) and one precursor without any carbon additions (NVP-noC-Pre). The experimentally determined carbon contents of the spray-dried precursors are 9.7, 3.4 and 0.1 wt.%. These values are somewhat larger than the theoretically expected (8.7, 2.6 and 0 wt.%) because the NVP reactants used already partially decompose during the synthesis process. Thus, the total mass of the NVP reactants is reduced which means that the relative carbon source content is increased. After calcination at 750 °C the carbon content of the different samples is 8.0, 1.1 and 0.1 wt.%, respectively. Compared to the nominal carbon contents, theoretically expected after the calcination (13.5, 3.9, and 0 wt.%), the experimental determined carbon contents are lower. The reason for the lower values is, on the one hand, that water and CO₂ are also released during the decomposition of the lactose and PAA, which means that some carbon is already lost. In addition, the carbon formed serves as a reducing agent in the reaction to NVP. The spray-drying process yields porous, hierarchically structured, more or less spherical granules with diameters of approximately 20 μm as can be seen from the SEM images in Figure 1. The porous

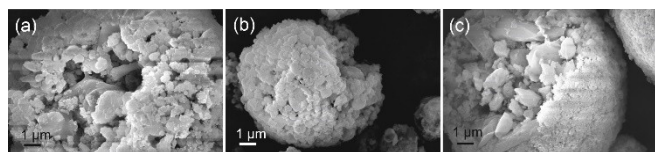


Figure 1. SEM images of the spray-dried NVP/C precursors, a) without carbon addition (NVP-noC-Pre), b) low amount of carbon (NVP-lowC-Pre) and c) high carbon content (NVP-C-Pre).

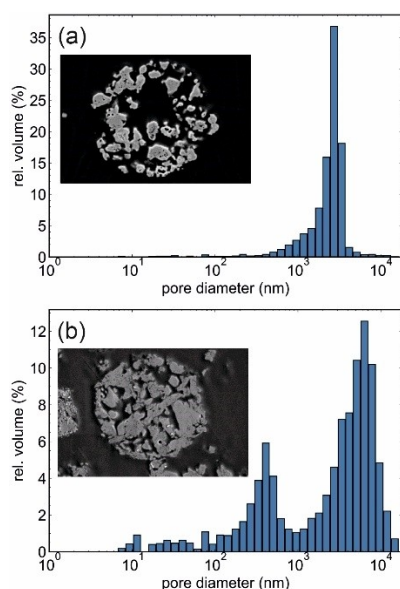


Figure 2. SEM cross sections and pore size distributions from Hg-porosimetry for a) NVP-lowC-750-Ar and b) NVP-C-750-Ar.

granule structures of the composites with low and high carbon content remain intact after calcination at 750 °C. The cross-sectional SEM images of the composites shown in Figure 2 clearly indicate the much larger porosity and larger pore sizes of the low carbon content sample NVP-lowC-750-Ar. The results of the Hg-porosity measurements (Figure 2) show a bimodal pore-size distribution for the high carbon content composite NVP-C-750-Ar. For NVP-lowC-750-Ar, it is not possible to distinguish between inter- and intra-granular pore space.

The X-ray diffraction patterns of NVP-lowC-750-Ar and NVP-C-750-Ar (Figure 3) confirm that after calcination at 750 °C the carbon containing precursors yield an almost phase-pure NVP material, which crystallizes in the rhombohedral R3c NASICON-type structure.^[26–28] In addition to the NVP phase a low amount of a V₂O₃ impurity phase can also be detected (~1 wt.%). The formed elemental carbon is present in an amorphous state. The chemical composition of the calcined materials is verified with ICP-OES (see Table S1). The results indicate a close to stoichiometric Na₃V₂(PO₄)₃ composition.

Rietveld refinement against the NVP-C-750-Ar X-ray powder data (Figure 4) yields lattice parameters of $a=b=8.7227(2)$ Å and $c=21.8379(9)$ Å. The estimated crystallite size calculated from a double-Voigt approach as implemented in the TOPAS software is 75 (3) nm.^[29] In contrast, the XRD pattern of the carbon free precursor shows no visible Bragg peaks, only a broad halo at ~13° 2θ, which demonstrates that the calcined synthesis product is amorphous. That means that the presence of carbon in the precursor is a prerequisite for obtaining a crystalline Na₃V₂(PO₄)₃ phase with this spray-drying based synthesis route. This will be discussed in more detail in the following sections.

Because of the denser microstructure of the granules of the carbon rich NVP/C composite the carbon rich precursor material was chosen for further investigations of the influence of calcination temperature and atmosphere on the morphological and structural properties.

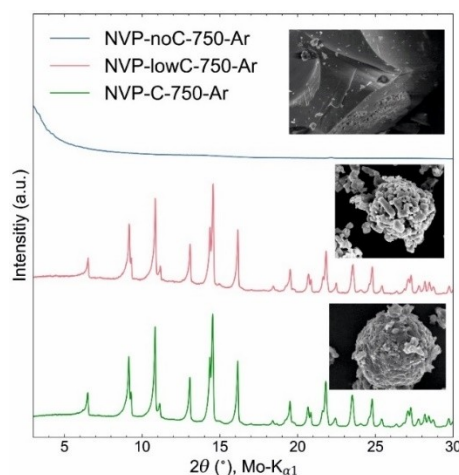


Figure 3. X-ray diffraction patterns of the NVP/C materials with varying carbon content calcined at 750 °C under argon.

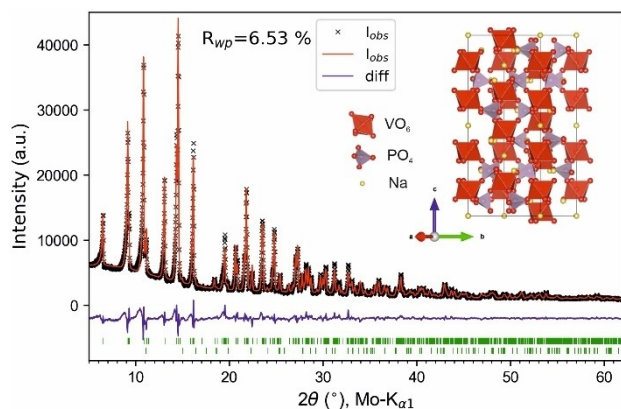


Figure 4. X-ray diffraction pattern and Rietveld refinement result of the NVP-C-750-Ar composite. The upper tic marks refer to the NVP phase and the lower tics to V_2O_5 . The inset shows the NVP NASICON structure.

The carbon rich precursor NVP-C-Pre was calcined at temperatures between 750 °C and 950 °C in steps of 50 °C and the calcined NVP/C composites are labelled according to the applied calcination temperature, i.e. NVP-C-750-Ar, NVP-C-800-Ar, NVP-C-850-Ar, NVP-C-900-Ar and NVP-C-950-Ar. An addi-

tional calcination of this precursor was conducted at 850 °C in a reducing atmosphere (H_2 3%, Ar 97%) with the goal to reduce all vanadium in the sample to V^{3+} . The SEM microstructure images together with cross sections of the NVP/C composites are shown in Figure 5. The median granule sizes of all calcined materials determined by laser diffraction are very similar with values of about 20 μm and all granules exhibit an open porosity. With increasing calcination temperatures up to 900 °C the porosity increases from 34 to 44% while the carbon content decreases from 8.0 to 4.5 wt.%. This may be due to evolving carbonaceous gases during the high temperature calcination process. At 950 °C most of the carbon is thermally decomposed and the NPV-C-950C-Ar composite contains only a minor carbon content of 0.5 wt.%. At the same time sintering occurs which leads to a decreased porosity of approximately 19%. The change to a reducing Ar/ H_2 atmosphere during calcination at 850 °C changes the granule microstructure only slightly, but leads to an increase of the carbon content from 7.4 to 8.4 wt.%. The reason for this is that the reducing atmosphere means that less carbon is consumed as a reducing agent during synthesis. The carbon contents and microstructural parameters of all synthesized samples are summarized in Table S2. It should be noted here, that unambiguous correlations between the values

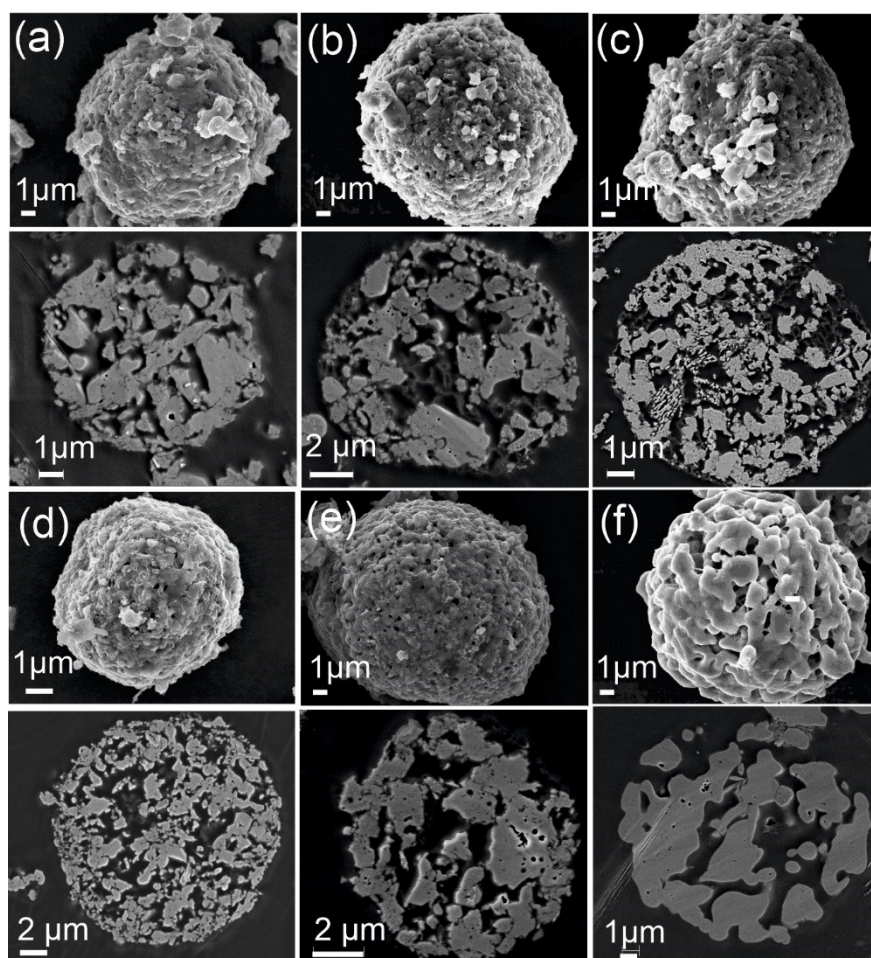


Figure 5. SEM images with the corresponding cross sections of the carbon rich NVP/C composite materials calcined at a) 750 °C, b) 800 °C, c) 850 °C, d) 850 °C Ar/ H_2 , e) 900 °C and f) 950 °C.

of the specific surface area and electrochemical performance cannot be made. The composites are multi-phase materials and the measured surface area is an effective area with contributions from both active NPV material and carbon. In addition, there are several phase transformation reactions accompanied with the formation of different phase and it is likely, that the microstructure (microporosity) is also altered during these reactions.

The X-ray diffraction patterns of the carbon rich, calcined composites are shown in Figure 6. For temperatures up to 850 °C the diffraction patterns are consistent with the NVP NASICON-type phase. At 750 °C a minor amount of approximately 1 wt.% of V_2O_3 can be detected. With increasing temperature this oxide phase disappears and new Bragg reflexes at 17.0° and 19.7° 2θ appear, which partially overlap with the 125 and 036 reflexes of NVP. These reflexes originate from the formation of a cubic vanadium carbide (VC) phase. The refinement of the lattice parameter of the vanadium carbide phases yields values of 4.135(1) Å and 4.138(1) Å and weight fractions of 2.0% and 3.3% for the 800 °C and 850 °C samples, respectively. The refined lattice parameters are smaller than those of stoichiometric VC. This indicates a carbon deficiency in the formed VC_{1-x} phases and hints to a chemical composition close to $VC_{0.7}$.^[30] Calcination at 850 °C under the reducing Ar/H_2 atmosphere has no significant effect on the phase composition compared to the sample calcined under pure argon.

At temperatures of 900 °C and 950 °C, a new set of reflexes can be observed in the diffraction patterns, which can be assigned to $Na_3V(PO_4)_2$. In addition, there are two reflexes of an unidentified phase at 18.1° and 20.1° 2θ . These results demonstrate that an almost phase pure NVP/C composite materials can be synthesized at temperatures up to 850 °C. At higher calcination temperatures the NVP NASICON structure is no longer thermodynamically stable and decomposes to different sodium vanadium phosphate phases with varying sodium contents.

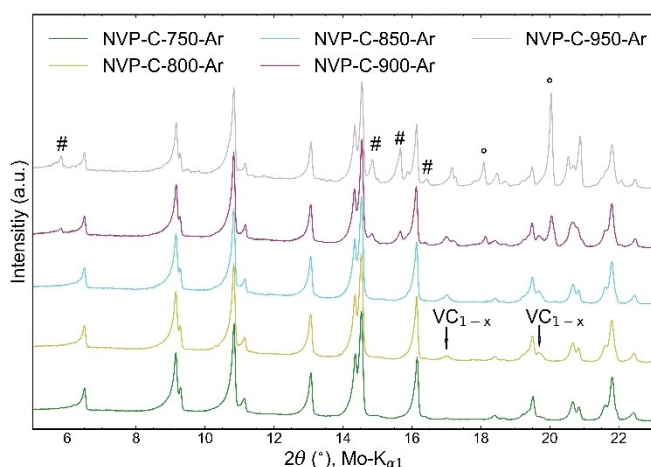


Figure 6. X-ray diffraction patterns of the NVP/C composites calcined at temperatures between 750 °C and 950 °C. (peaks marked with # are due to $Na_3V(PO_4)_2$, peaks marked with ° belong to an unidentified phase).

As can be seen from the SEM cross section of the composite granules in Figure 5 the particle sizes of the NVP are still relatively large with an inhomogeneous porosity distribution within the single spherical granules. Therefore, in an attempt to optimize the granule microstructure in terms of particle size and porosity a second milling step was introduced in the process. An agitator ball mill with small zirconia milling balls (\varnothing 200 μ m) were used for this additional process step, followed by spray-drying and calcination at 850 °C under a reductive Ar/H_2 atmosphere. The SEM cross section of this composite is shown in Figure 7. It is evident that the additional milling process leads to a much finer microstructure with smaller primary particles and a homogeneous distribution of the porosity within the granules. The diameter of the granules is reduced from approximately 17 to 10 μ m and the pore sizes are significantly decreased from 387 to 76 nm. At the same time, the porosity increases from 36% to 52% whereas the remaining carbon content of both composites is approximately 8 wt.%. Finally, there is a large increase of the specific BET surface area from 34 to 120 m^2/g . The large reduction of the pore sizes within the secondary particles originates from the spray-drying process. After the second milling step, the NVP particles are much smaller. Spray-drying of such small particles leads to granules with a low interparticle volume and in addition, the small particles preferably add at the border of the granules.^[31] After calcination, these small pore sizes are preserved.

Thermal analysis of the precursor decomposition

The pyrolysis of the spray-dried precursor materials involves several reaction steps such as the thermal decomposition of the used educts, the formation and crystallisation of the product phase as well as crystal growth. We investigated the thermal decomposition with the aid of simultaneous TG/DSC coupled with FTIR spectroscopy (Figure 8). It should be noted, that after the spray-drying process Na_2CO_3 has already been transformed to the corresponding oxide and hydroxide phases. As expected, the carbon-rich precursors show higher mass losses in the TG curves. Mass loss starts well below 200 °C with the evolution of CO_2 , NH_3 and H_2O . NH_3 gas originates from the decomposition of NH_4VO_3 and $NH_4H_2PO_4$ precursors whereas the release of CO_2 and H_2O is related to the decomposition of the ammonium containing reactants as well as the carbon sources β -lactose

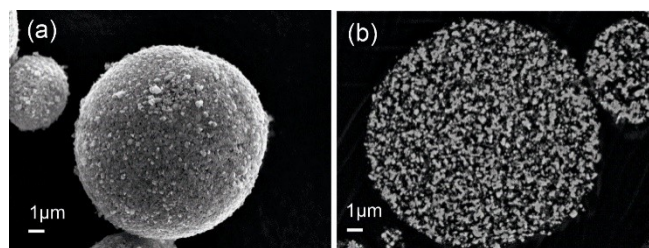


Figure 7. a) SEM image and b) cross section of the carbon rich NVP/C precursor calcined at 850 °C under a reducing Ar/H_2 atmosphere and an additional ball-milling step (NVP-C-850- Ar/H_2 -fine).

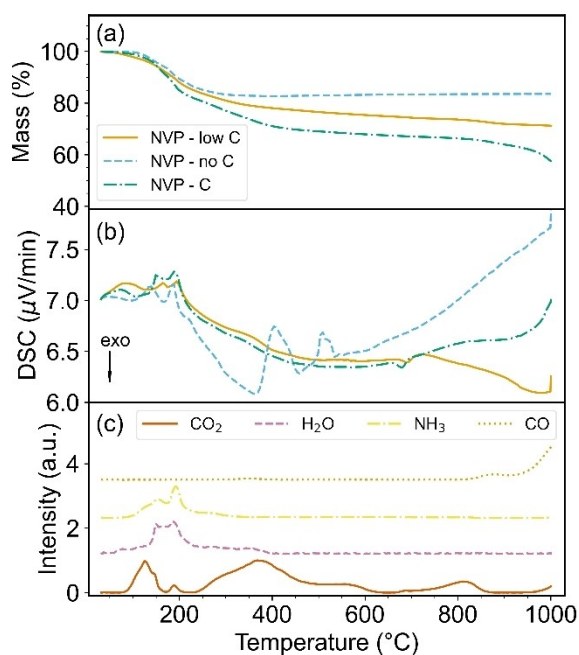
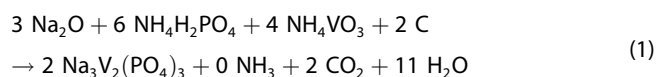


Figure 8. Simultaneous TG/DSC curves (a), (b) of the different NVP/C precursor materials and (c) traces of the evolved gases from the coupled FT-IR spectroscopy during thermal decomposition of NVP-C-Pre.

and PAA. The temperature increase up to 400 °C leads to a second decomposition step with the release of more CO₂, as can be seen from the CO₂ trace of the FTIR spectra in Figure 8(c), and a further loss in mass. The carbon containing precursors exhibit a continuous mass loss throughout the complete temperature range whereas the mass of the carbon free precursor stays almost constant at temperatures higher than 500 °C. This means that the thermal decomposition of the reactants is finished at approximately 500 °C. Up to this temperature, the decomposition of the carbon sources also leads to the formation of elemental carbon under the inert argon atmosphere. The mass loss of the carbon containing precursors associated with the higher temperatures is due to the beginning oxidation of the formed carbon to CO₂. Another large mass loss step in the TG curve of the carbon rich precursor can be observed at 850 °C. From the inspection of the FTIR traces, it is evident that this mass loss originates from the liberation of CO. This CO gas release can be associated with the decomposition of the NVP phase to Na₃V(PO₄)₂ and an unidentified phase in accordance with the XRD results. The newly formed elemental carbon is essential for the formation of the NVP phase because some part of the carbon reduces the vanadium from the +V to the +III oxidation state according to the following reaction equation (Eq. 1):



Crystallization of the product NVP phase can be observed at around 750 °C for both carbon containing precursor materials based on the small exothermic DSC peak.^[32] This peak does not

occur in the DSC signal for the carbon free precursor, but some endothermic effects are visible in the temperature range between 400 and 500 °C. Thus, it seems that the carbon free precursor undergoes a melting process and the NVP product phase is not formed. This is in accordance with the diffraction pattern of the calcined carbon free precursor, which only shows amorphous features. A different synthesis approach is reported by Chotard et al.,^[33] where V₂O₃ is used as a Vanadium containing educt phase instead of NH₄VO₃. In this synthesis route no carbon is necessary as a reducing agent because Vanadium is already in the +III oxidation state. An advantage of our synthesis is the in-situ formation of a carbon matrix, which enhances the electronic conductivity of the composite. Carbon free NVP materials on the other hand exhibit poor electrochemical performance.^[34]

Electrochemical performance

In order to decipher the influence of the processing parameters on the electrochemical performance of the NVP/C composites, electrochemical measurements were performed on CR2032-type coin cells between 2.3 V-3.9 V. The results of the rate-capability tests of the materials with the different amounts of carbon, which were calcined at 750 °C are depicted in Figure 9(a-b). NVP-lowC-750-Ar exhibits an initial capacity of 104 mAh/g at 0.15 C whereas NVP-C-750-Ar has a lower capacity of 92 mAh/g. The lower capacity may be due to the higher carbon content and a thicker, denser carbon coating on the electrochemical active NVP particles. These dense carbon layers may inhibit ionic conductivity and therefore some parts of the NVP material may become electrochemically inactive.^[34] The rate performance of NVP-C-750-Ar is better than that of NVP-lowC-750-Ar (see Figure 9(b)). The reason for the poor rate capability of the low carbon content material is the higher internal resistance of the cell, which has a large impact on the charging behaviour, especially at higher C-rates. This becomes obvious, when the charge-discharge curves of the two composites are compared (Figure S1). The polarisation at 15 C of the carbon-rich composite is lower than that of NVP-lowC-750-Ar. Therefore, in the applied voltage window, there is almost no charging of the NVP-lowC-750-Ar material. Reasons for the high resistance are the larger primary particles with larger diffusion path lengths, leading to a lesser exploitation of the active material, as well as the lower electronic conductivity within the secondary particles due to an inhomogeneity and lower amount of the carbon matrix. NVP-C-750-Ar outperforms NVP-lowC-750-Ar in terms of cycle stability. While the latter shows a capacity of 74 mAh/g (72% of the initial capacity) after 400 cycles, the former still has a capacity of 86 mAh/g (94%).

The influence of the calcination temperature on the cycling stability and rate capability is shown in Figure 9(c-d). During the rate capability test NVP-C-850-Ar exhibits the highest capacity at 15 C with 70 mAh/g followed by NVP-C-800-Ar with a capacity of 63.2 mAh/g. The difference in terms of capacity between NVP-C-850-Ar and NVP-C-800-Ar increases with the C-rate. NVP-C-750-Ar and NVP-C-900-Ar show capacities of

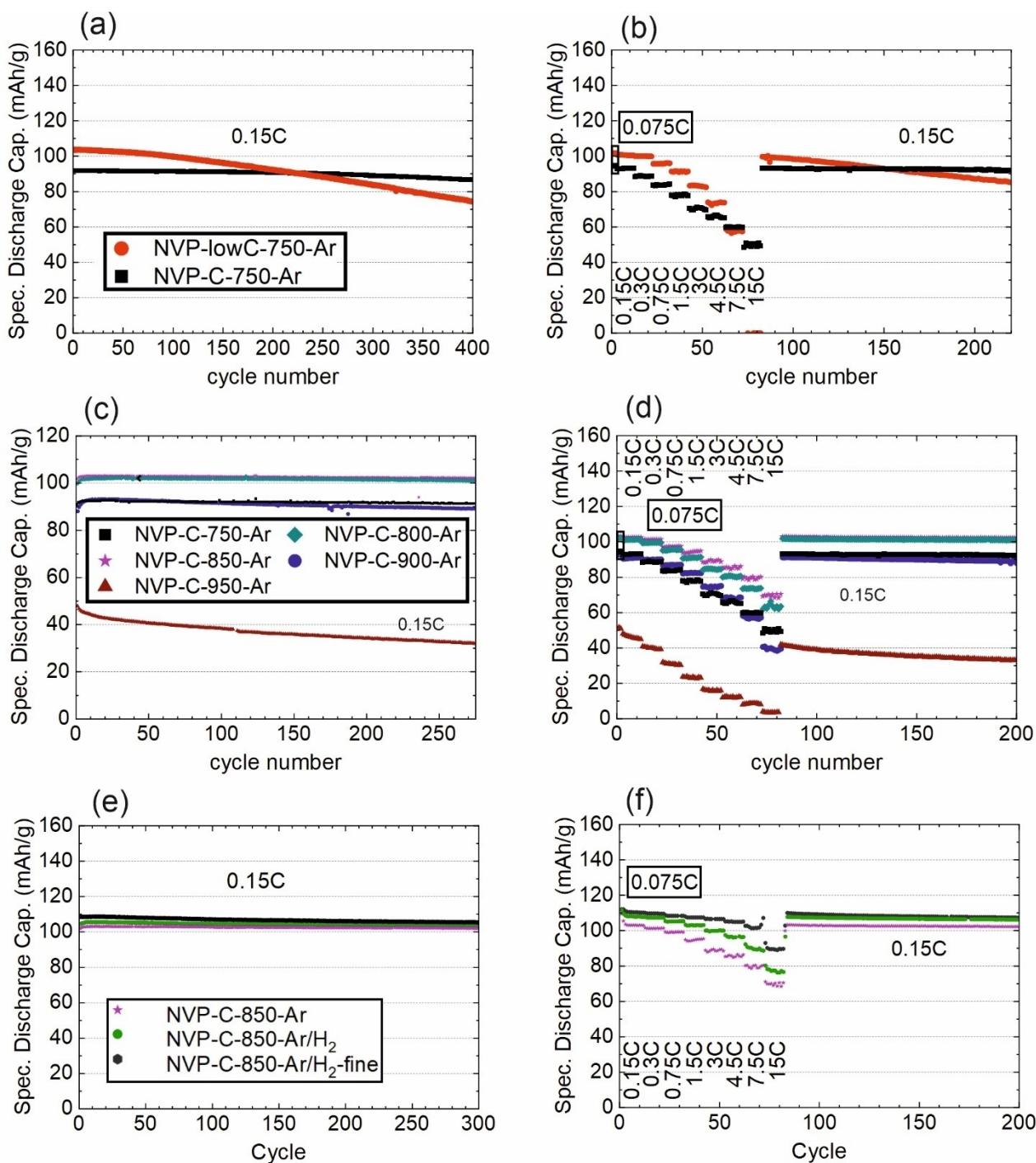


Figure 9. Influence of different processing parameters on the electrochemical cycling stability and rate capability tests of the NVP/C composites, a-b) variation of the carbon content, c-d) calcination temperature, e-f) calcination atmosphere and particle size.

49.4 mAh/g and 39.5 mAh/g at a C-rate of 15 C. Whereas NVP-C-950-Ar with the lowest carbon content of 0.4 wt.% still exhibits some capacity, NVP-lowC-750-Ar with a slightly higher carbon content of 1.1 wt.% is electrochemically inactive. This different behaviour is due to the microstructure of NVP-C-950-Ar. NVP-C-950-Ar is more compact compared to NVP-lowC-750-Ar and still has a thin, interconnected carbon coating on the particle surface.

During the stability test with a constant C-rate of 0.15 C NVP-C-950-Ar exhibits the lowest initial capacity of 47.4 mAh/g, which decreases to 31.6 mAh/g after 275 cycles. This corresponds to a capacity retention of around 66.6%. NVP-C-850-Ar exhibits the highest capacity with 103.2 mAh/g, closely followed by NVP-C-800-Ar with 102 mAh/g. Both composites have a capacity retention of approximately 99% after 275 cycles. NVP-C-750-Ar and NVP-900-Ar exhibit a lower capacity of 91.9 mAh/g

g and 93.1 mAh/g with a capacity retention of 98.4% and 95.8% (Figure 9(a)). The results of the rate capability tests demonstrate that a certain amount of carbon is necessary for high capacity retention. NVP-C-900-Ar and NVP-C-950-Ar with carbon contents of 4.5 and 0.4 wt.%, exhibit the lowest stability, whereas the other composites have similar capacity retentions and share almost the same carbon content of 7–8 wt.%. This amount of carbon seems to be a good compromise between high initial capacity and cycling stability. These results clearly demonstrate that the calcination temperature is an important process parameter for the electrochemical performance because it has a strong influence on the final phase composition of the NVP/C composite and on the microstructure and type of the carbon matrix, as was also shown in earlier studies.^[35,36] When the calcination temperature is higher than 900 °C the NVP phase thermally decomposes and the carbon is oxidised to CO and CO₂.

A change of the calcination atmosphere to a mixture of Ar/H₂, which leads to reducing conditions during calcination, gives a higher initial capacity of 106 mAh/g and a capacity retention of 98.4% after 275 cycles for composite NVP-C-850-Ar/H₂. The rate capability of this composite is also increased (Figure 9(e-f)) with a value of 77 mAh/g at 15 C. The better electrochemical performance of this composite may be due to a higher part of vanadium, which is reduced from oxidation state +V to +III as well as an increased carbon content (8.4 wt.%) and therefore higher electronic conductivity.

In addition to the function as a reducing agent for vanadium, the formed carbon not consumed during this reduction process, serves as an electronic conductivity additive within the secondary particles. Several synthesis approaches for the realization of conductive carbon matrixes exist, which result in different types of carbon matrixes. The type of the conductive matrix and the spatial distribution of carbon within the composite have a significant influence on the electrochemical performance.^[37] An advantage of the in situ formation of the conductive carbon matrix from the thermal decomposition of the carbon containing precursors during synthesis, is the inhibition of particle growth of the NVP phase yielding nano NVP/carbon composites. This nanodesigned microstructure leads to a homogeneous redox reaction throughout the complete secondary particles without any inactive regions. On the contrary, subsequent coating processes after the initial synthesis step of NVP particles often yield limited improvements of the electrochemical performance because the coating is fragmentary and electrochemical inactive regions remain within the composite.^[38]

The reduction of the particle size of the cathode active NVP material further improves the initial capacity up to 108 mAh/g with a capacity retention of 97.6% after 225 cycles (see Figure 9(e-f)). The fine particle size of the composite together with the increased porosity and specific surface area enhance the penetration of the electrolyte throughout the electrode and at the same time, the diffusion paths are shorter. Therefore, this material reaches the highest observed capacity of 91 mAh/g at 15 C with a comparably good cycling stability. The pore size diameters of NVP-C-850-Ar/H₂-fine are the smallest in the

investigated series of NVP/carbon composites. Nevertheless, this value seems large enough for a complete electrolyte penetration throughout the secondary particles so that the electrochemical performance is not affected.

Conclusions

To summarize, we have performed a comprehensive investigation of the influence of process parameters on the electrochemical properties of hierarchically structured NVP/C composite materials. We demonstrated the need of a carbon containing precursor such as PAA or β -lactose in the spray-drying synthesis process. The newly formed elemental carbon acts as a reducing agent for vanadium +V and reduces the vanadium to the +III oxidation state during calcination. Low carbon contents of approximately 3 wt.% are too low to boost the electronic conductivity of the composite and resulted in a low cycling stability and fast capacity fading. Higher carbon contents up to 10 wt.% drastically improved the electrochemical performance of the NVP/C composites. The best electrochemical performance was observed for a finely ground material calcined at 850 °C under a reducing Ar/H₂ atmosphere. Ar/H₂ acts as an additional reducing agent for vanadium and increases the capacity because of a more complete reduction of vanadium ions. Increasing the calcination temperature above 900 °C provokes in the onset of thermal decomposition of the NVP NASICON structure. An advantage of the presented combination of a spray-drying synthesis and an agitator ball milling process is the possibility to upscale this process to larger synthesis batch sizes, which is a prerequisite for next-generation large-scale batteries for industrial applications.

Experimental Section

Synthesis of Na₃V₂(PO₄)₃/C composites

For the synthesis of the NVP/C particles, we refer to the synthesis of Secchiaroli et al.^[39] Ammonium metavanadate (NH₄VO₃, Honeywell), sodium carbonate (Na₂CO₃, VWR) and ammonium dihydrogen phosphate (NH₄H₂PO₄, VWR) were dispersed in absolute ethanol (C₂H₆O, VWR) in a molar ratio of 4:3:6. Additionally polyacrylic acid ([C₃H₄O₂]_n, Sigma Aldrich) and β -lactose (C₁₂H₂₂O₁₁, Sigma Aldrich), which act as carbon sources after pyrolysis, were added for the synthesis of carbon containing precursors. The precursors are labelled as NVP-noC-Pre, NVP-lowC-Pre and NVP-C-Pre. The labels refer to the carbon content of the precursor materials, i.e. carbon free, 5 wt.% and 16.7 wt.% of carbon sources. The as prepared suspension was milled for 5 hours in a planetary ball mill with ZrO₂ grinding balls (ϕ 3 mm). After removing the grinding balls by sieving and dilution with ethanol, spray-drying was performed with an inlet-temperature of 150 °C and an outlet-temperature of 95 °C in a spray-dryer (Mobile Minor, GEA). The powder was finally sieved using a 50 μ m sieve. The synthesized precursor materials were calcined at 700 °C, 750 °C, 800 °C, 850 °C, 900 °C and 950 °C under inert argon atmosphere and under a reductive argon-hydrogen atmosphere (H₂ 3%, Ar 97%). A pre-calcination step at 400 °C for 4 h was used to generate a controlled gas evolution. Afterwards the powders were heated to the final temperature and kept at this

temperature for 12 h, before cooling to room temperature. For the calcination a heating and cooling rate of 5 °C/min was used. The calcination temperature and atmosphere is included in the labels of the investigated materials, for example NVP-C-750-Ar for the 16.7 wt.% of carbon containing sample calcined at 750 °C under an argon atmosphere. The NVP-C precursor material was grinded in a second milling step with an agitator ball mill by the use of ZrO₂ milling balls (ø 200 µm) in a suspension in ethanol to create smaller particles. After removing the milling balls the suspension was diluted with ethanol and spray-dried. The as received granules were calcined under reductive conditions at 850 °C with the aforementioned calcination program to get the NVP-C-850-Ar/H₂-fine sample.

Material characterization

X-ray diffraction (XRD) of the synthesized powders was performed on a Stoe Stadi P diffractometer with monochromatic Mo-K_{α1} radiation from 3 to 60° 2θ in Debye-Scherrer geometry in 0.5 mm sealed glass capillaries. The morphology of the particles was investigated with scanning electron microscopy (SEM) with a Zeiss Supra 55. Specific surface area was measured via nitrogen sorption analysis (NSA, Gemini VII 2390a, Micromeritics) by using the Brunauer-Emmett-Teller (BET) equation in the linear pressure range. Internal porosity was measured by mercury intrusion porosimetry (CEI Pascal 1.05, Thermo Electron). The internal porosity P was calculated according to (Eq. 2)

$$P = \frac{V_p}{V_p + 1/\rho}, \quad (2)$$

where V_p is the inner specific pore volume, between 4 nm and 774 nm, and ρ is the measured density. The density of NVP was measured with He-pycnometry (Porotec pycnomatoc-ATC) and is 2.84 g/cm³. Particle sizes of the powders were determined via laser diffraction (Horiba LA950, Retsch Technology). Inductively coupled plasma-optical emission spectroscopy (ICP-OES) was used to check the overall composition of the processed materials (iCAP 7600 Duo, Thermo Fisher Scientific). The carbon content of the powders was measured via a CS-analyser. The thermal decomposition of the precursors were investigated by thermogravimetric analysis in a Netzsch STA 449 Fe Jupiter simultaneous thermal analyser coupled with a Fourier-transform infrared spectrometer (Bruker Vertex 70). Heating rates of 5 °C/min up to a temperature of 1000 °C and an argon atmosphere were used.

Electrochemical characterization

Electrodes were prepared by mixing the NVP/C-powders with polyvinylidene fluoride (PVDF, Sigma Aldrich) and the conductive carbon additive TIMCAL-C65 with a weight ratio of 80:10:10 in a Speed Mixer DAC 150 by Hausschild. The obtained paste was doctor bladed on an aluminium foil with a gap size of 200 µm (Erichsen Coatmaster 510). The cast films were dried in two steps, first for 30 minutes at 80 °C in air and afterwards at 120 °C under vacuum for 12 hours. Thereby mass loadings of the active material between 1.3 and 4.6 mg/cm² were achieved. Electrodes were punched out with a diameter of 12 mm and applied as working electrodes in CR2032 coin cells with a glassfiber separator (16 mm diameter, Whatman GF/C), and a sodium counter electrode (12 mm diameter). A 1 M solution of NaClO₄ in a mixture of EC, DMC and FEC in a volumetric ratio of 9:9:2 was applied as electrolyte. The coin cells were assembled in a glovebox filled with argon. Rate

capability and galvanostatic cycling with potential limitation (GCPL) cell tests were carried out in a galvanostat from Arbin in a voltage window of 2.3 V-3.9 V vs Na⁺/Na with currents ranging from 50 µA to 10 mA. The C-rate is calculated by the theoretical capacity of Na₃V₂(PO₄)₃ which is approximately 118 mAh/g. For the calculation of the specific capacity of the materials, the mass of residual carbon after calcination is subtracted from the active material mass.

Acknowledgements

This work contributes to the research performed at CELEST (Center of Electrochemical Energy Storage Ulm-Karlsruhe) and was funded by the Deutsche Forschungsgemeinschaft (DFG, German Research Foundation) under Germany's Excellence Strategy – EXC 2154 – Project number 390874152. The authors are grateful for the ICP-OES measurements, performed by Dr. Thomas Bergfeldt from the IAM-AWP at KIT. Open Access funding enabled and organized by Projekt DEAL.

Conflict of Interests

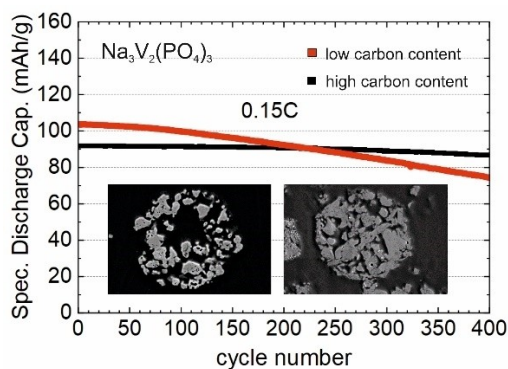
The authors declare no conflict of interest.

Data Availability Statement

The data that support the findings of this study are openly available in Zenodo at <https://doi.org/10.5281/zenodo.10278224>, reference number 10.5281/zenodo.10278224.

Keywords: energy storage · sodium-ion batteries · NASICON · electrode materials · carbon

- [1] D. Kundu, E. Talaie, V. Duffort, L. F. Nazar, *Angew. Chem. Int. Ed.* **2015**, *54*, 3432.
- [2] H. Kim, Z. Ding, M. H. Lee, K. Lim, G. Yoon, K. Kang, *Adv. Energy Mater.* **2016**, *6*, 1600943.
- [3] M. Chen, Q. Liu, S.-W. Wang, E. Wang, X. Guo, S.-L. Chou, *Adv. Energy Mater.* **2019**, *9*, 1803609.
- [4] F. Risacher, B. Fritz, *Aquat. Geochem.* **2009**, *15*, 123.
- [5] B. Simon, S. Ziemann, M. Weil, *Resour. Conserv. Recycl.* **2015**, *104*, 300.
- [6] J. Y. Hwang, S. T. Myung, Y. K. Sun, *Chem. Soc. Rev.* **2017**, *46*, 3529.
- [7] G. Klinser, R. Zettl, M. Wilkening, H. Krenn, I. Hanzu, R. Würschum, *Phys. Chem. Chem. Phys.* **2019**, *21*, 20151.
- [8] J. Kang, S. Baek, V. Mathew, J. Gim, J. Song, H. Park, E. Chae, A. K. Rai, J. Kim, *J. Mater. Chem.* **2012**, *22*, 20857.
- [9] C. Xu, J. Zhao, Y.-A. Wang, W. Hua, Q. Fu, X. Liang, X. Rong, Q. Zhang, X. Guo, C. Yang, H. Liu, B. Zhong, Y.-S. Hu, *Adv. Energy Mater.* **2022**, *12*, 2200966.
- [10] P. Li, M. Gao, D. Wang, Z. Li, Y. Liu, X. Liu, H. Li, Y. Sun, Y. Liu, X. Niu, B. Zhong, Z.-G. Wu, X. Guo, *ACS Appl. Mater. Interfaces* **2023**, *15*, 9475.
- [11] X. Liu, G. Feng, Z. Wu, Z. Yang, S. Yang, X. Guo, S. Zhang, X. Xu, B. Zhong, Y. Yamauchi, *Chem. Eng. J.* **2020**, *386*, 123953.
- [12] J. Li, B. Peng, Y. Li, L. Yu, G. Wang, L. Shi, G. Zhang, *Chem. Eur. J.* **2019**, *25*, 13094.
- [13] L. Si, Z. Yuan, L. Hu, Y. Zhu, Y. Qian, *J. Power Sources* **2014**, *272*, 880.
- [14] W. Shen, C. Wang, Q. Xu, H. Liu, Y. Wang, *Adv. Energy Mater.* **2015**, *5*, 1400982.
- [15] S. Tao, X. Wang, P. Cuie, Y. Wang, Y. A. Haleem, S. Wei, W. Huang, L. Song, W. Chu, *RSC Adv.* **2016**, *6*, 43591.



Hierarchically structured $\text{Na}_3\text{V}_2(\text{PO}_4)_3/\text{carbon}$ composite materials are synthesized via a spray-drying process. By systematically varying the processing parameters such as the calcination temperature and atmosphere, carbon

content and ball-milling parameters, the morphology and microstructure of the composite can be adjusted, which finally yields optimized electrochemical performance.

*M. Häringer, Dr. H. Geßwein, N. Bohn, Prof. H. Ehrenberg, Dr. J. R. Binder**

1 – 10

Influence of Process Parameters on the Electrochemical Properties of Hierarchically Structured $\text{Na}_3\text{V}_2(\text{PO}_4)_3/\text{C}$ Composites

